

ICONN 2015 [4th - 6th Feb 2015]

International Conference on Nanoscience and Nanotechnology-2015

SRM University, Chennai, India

Synthesis of TiO₂ nanotubes from prepared TiO₂ nanoparticles by hydrothermal route and dye sensitized solar cell characteristics

G. Arthi¹, J. Archana², M. Navaneethan², S. Ponnusamy¹, Y. Hayakawa²,
C. Muthamizhchelvan^{1*}

¹Department of Physics and Nanotechnology, SRM University, Kattankulathur 603203, Tamil Nadu, India.

²Research Institute of Electronics, Shizuoka University, 3-5-1 Johoku, Naka-ku, Hamamatsu, Shizuoka 432-8011, Japan.

Abstract : A simple hydrothermal reaction among TiO₂ nanopowders and alkaline solution has been developed to synthesize low dimensional titanate nanostructures. The morphologies of the obtained nanomaterials depend on the process parameters: the structure of starting material, the nature and concentration of alkaline solution, reaction temperature and time, which suggests that the nanostructure synthesis could be controllable. Here we made an attempt to synthesize titanate nanotubes via hydrothermal reaction of TiO₂ crystals of anatase and NaOH solution in the range of 110-160°C. It seems to be titanate nanotubes obtained only at temperature 110°C with the diameter 10 nm. The phase of the obtained TiO₂ nanostructures were analyzed by X-ray diffraction (XRD) and Raman spectroscopy. The morphologies of the nanostructures were analyzed by several methods including Scanning electron microscope (SEM), High resolution transmission electron microscope (HRTEM). UV-Diffusion reflectance spectra (UV-DRS). The surface area and pore diameter of nanotubes were determined by Brauner-Emmett-Teller (BET) method. The flexible DSSC with light-to-electric energy conversion efficiency of 2.38% was achieved for optimized nanotubes under a simulated solar light irradiation of 100mWcm⁻².

Keywords: Titania, Hydrothermal treatment, Nanomaterials, Nanotubes, Dye-sensitizer.

1. Introduction

Dye sensitized solar cells have attracted immensely as an economical energy conversion device because of their low cost and high efficiency^{1,2}. Engineering materials such as ZnO, SnO₂, CdS, and TiO₂ contributed their major part in various applications like photocatalysis, environmental cleaning and protection, gas sensing, lithium ion batteries and solar cells. Among various metal oxide semiconductors TiO₂ have gained great interest because of its inconceivable performance in dye sensitized solar cells³⁻⁶.

A typical DSSC device is made up of working electrode (photoanode), counter electrode and electrolyte. Different kinds of morphologies of the photoanode have been synthesized to improve the efficiency of the device. In DSSC, TiO₂ nanoparticles are working as photoanode⁷⁻⁹. To avoid the disadvantages like

ohmic loss, grain boundaries and recombination, 1 – dimensional TiO₂ nano structures are used as photoanodes instead of TiO₂ nanoparticles. Hence the 1-dimensional structures such as nanotube, nanowire, and nanorod are ideal materials for device fabrication¹⁰⁻¹⁶. 1-dimensional TiO₂ nano structures have been prepared by various established methods: 1) template 2) surfactant directed synthesis 3) alkali treatment under hydrothermal conditions¹⁷⁻²³. The alkali treatment is an effective method to synthesis nanotubes under moderate hydrothermal conditions. The reaction temperature and reaction time are the two main factors which have control over the structure of morphology^{24, 25}.

In the present study we explored the formation of anatase TiO₂ nanotubes by hydrothermal growth using TiO₂ nanoparticles. The growth parameter for preparation of TiO₂ nanotubes by inexpensive route has also been presented. Optimized condition for the synthesized products has been characterized by XRD, UV, TEM, BET, and IV.

Karthik kinhal et al., had achieved the efficiency of 11.2 % in DSSC with the candidate of TiO₂ nanoparticles, as photoanode. Thus the performance of TiO₂ nanoparticles is still limited, due to the multiple disadvantages as described above. Therefore the use of 1-dimensional nano structures will definitely lead to a great improvement in efficiency due its better properties like electron diffusion length, high dye absorption, fast electron transport, and no grain boundaries.

2. Experimental

2.1 Preparation of TiO₂ nanoparticles

TiO₂ nanopowders were prepared via hydrothermal method using Tetra-n-butyl-titanate and deionized water as the starting materials. The concentration of the above chemicals were (the volume ratio of tetra-n-butyl titanate: deionized water) 1:6. Tetra-n-butyl titanate was added drop wise into the deionized water. The obtained gel was then autoclaved at 105°C for 10 hrs. The precipitate was washed with distilled water. Then the powder was dried in oven for 24 hours and then calcined at 450 °C.

2.2 Preparation of TiO₂ nanotubes from as prepared TiO₂ nanoparticles:

In a typical preparation procedure 0.3 g of prepared TiO₂ white power was placed into a Teflon-lined autoclave of 100 ml capacity. 10M NaOH was mixed with 20 ml of distilled water and stirred for 1 hour. The solution was transferred into autoclave and maintained at 110 °C for 24 h. Then the autoclave was allowed to cool naturally to room temperature. The obtained products were collected and washed with HCl aqueous solution for several times until the pH value turned to 7. The products were then annealed at 400 °C in air for 2h.

1.5 g of prepared TiO₂ nanotubes was mixed with ethanol and 1 drop of Triton-X and ground well. The mixture was then ultrasonicated for approximately 30 minutes. The mixture was sprayed onto the FTO substrate using a spray deposition technique. The resulting film was annealed at 450 °C for 2 h and then immersed for 12 h in an ethanolic solution containing 0.03M ruthenium (N-719) for dye adsorption. The dye-sensitized photoanode was clamped with a platinum electrode and filled with iodide redox electrolyte (0.6 M dimethyl propylimidazolium iodide, 0.1 M LiI, 0.01 M iodine, 0.5 M 4-tertbutylpyridine in acetonitrile).

2.3 Characterization methods

The structural analyses of the TiO₂ samples were examined with powder X-ray diffraction (XRD) using a X' Pert Powder XRD System equipped with Cu-K α radiation. The data were collected for scattering angles (2 θ) ranging between 10° to 80° with a step size of 0.2°. The external features and morphology of the samples were detected by scanning electron microscopy (SEM) using JEOL JSM-6700F and Transmission electron microscope. UV-visible (UV-Cary 5E) spectrophotometer was used to obtain optical absorption spectra of the samples.

Surface area of the samples was analyzed using a (BET) Micromeritics ASAP 2020 V3.00 H. Pore structure of the derived TiO₂ nanotubes was characterized by N₂ adsorption using an appropriate apparatus. Surface area of the samples was determined from the Brauner-Emmett-Teller (BET) equation. The pore size distribution was analyzed using the Barret-Joyner-Halanda (BJH) method.

3. Results and discussion

Figure.1 (a) shows the X-ray diffraction patterns of the as-synthesized TiO₂ nanoparticles (TNP) (b),(c) and (d) shows the XRD of TiO₂ nanotubes (TNT) prepared at 110 °C, 130 °C, 160 °C respectively. From fig. 1(a) the diffraction peaks indicate the formation of TNPs with a pure anatase phase with high intensity. In fig. 1(b) shows, the peaks are corresponding to anatase phase. Diffraction peaks in TNTs are weaker and low intensity than those in the TNPs. This is because of NaOH treatment on TNPs. At the moment of NaOH mixed with the TiO₂ nanoparticles, NaOH would rupture the Ti-O-Ti bonds, causing a lower crystallinity in the TNTs. When the temperature increased to 130 °C the phase transformation occurs from anatase to rutile phase.

Figure.1 (e), (f) and (g) shows Raman spectra of samples prepared at 110°C, 130°C, 160°C respectively. From figure 1(e) clearly shows the Raman peaks corresponding to the anatase phase of TiO₂ nanotubes prepared at 110 °C. The strong Raman peaks around 144, 197, 400, 515, and 640 cm⁻¹ were assigned to the anatase structure.

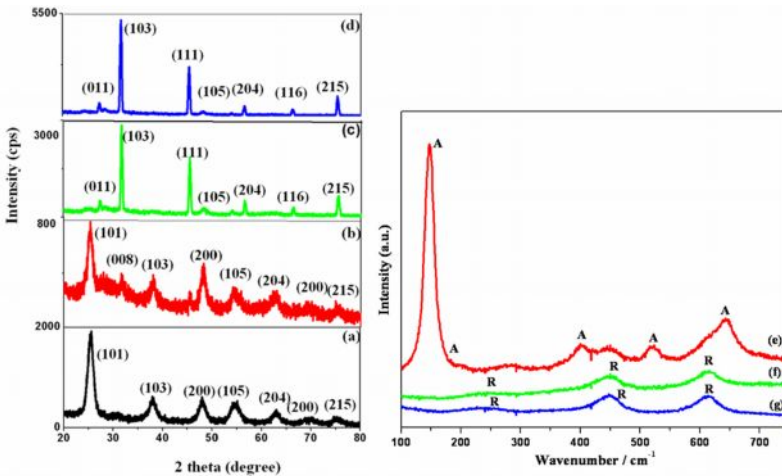


Figure.1 (a) shows X-ray diffraction pattern of the as-synthesized TiO₂ nanoparticle, (b), (c) and (d) shows the XRD of TiO₂ nanotubes prepared at 110°, 130°C, 160°C. Figure.1 (e, f, g) shows Raman spectra of samples prepared at 110 °C, 130 °C , 160 °C .

While the temperature was increased to above 130 °C and 160 °C the anatase phase began to transform to the rutile phase. Raman peaks around 235, 447 and 612 cm⁻¹ assigned to the rutile phase of TiO₂ from figure 2 (f) and 2 (g)²⁵. Peaks representing the anatase and the rutile form of TiO₂ are labeled A and R, respectively.

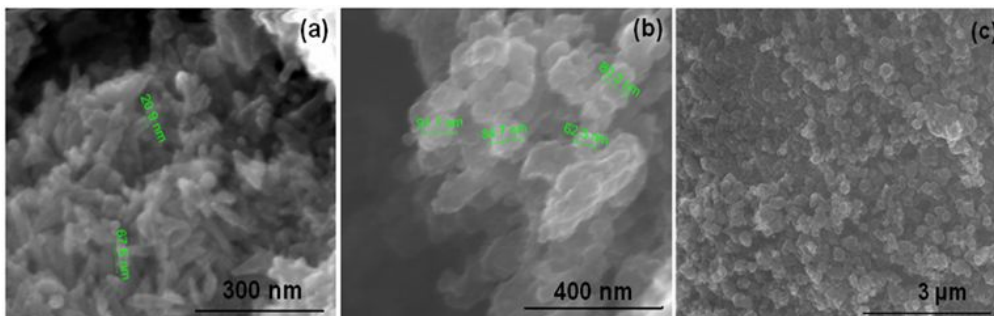


Figure. 2 (a), (b) and (c) shows the SEM images of TiO₂ nanotubes grown at 110°, 130°C, 160°C.

Fig 2 (a),(b) and (c) shows a sequence of SEM images taken from the samples grown at 110 °C, 130 °C, 160 °C. From image 3(a) observed that the TiO₂ nanotubes grown only at 110 °C, with the diameter around 10 nm and length 60 nm. Upon an increase of hydrothermal temperature (130 °C) the nanotubes were started to disintegrate with the particle size of 80-90 nm and some of them aggregated together shows in figure (b). At 160 °C the nanotubes were fully converted into spherical particles with sizes of 150-180 nm shows in figure (c).

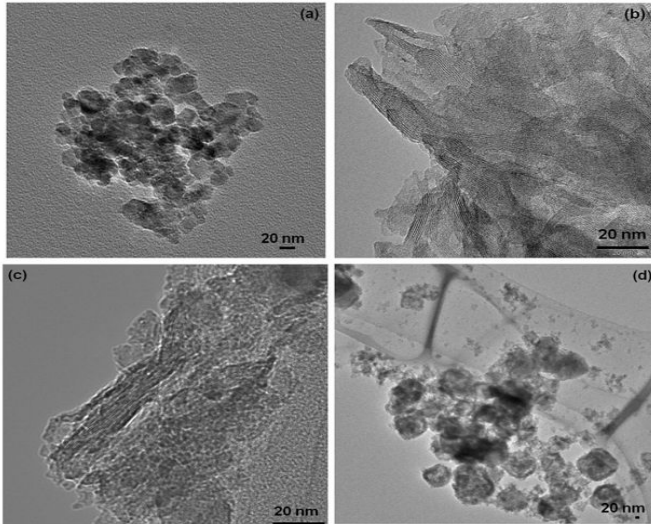


Figure. 3 (a) shows TEM images of TiO₂ nanoparticles, (b), (c) and (d) shows the TEM images of TiO₂ nanotube prepared at 110°, 130°C, 160°C

Figure.3 (a) shows the TEM images of TiO₂ nanoparticles, (b), (c) and (d) shows the TEM images of samples prepared at 110 °C, 130 °C, 160 °C. Fig. 3 (b) shows the TEM image of the sample which was grown at 110 °C for 24 h, showing a pure tube-like structure. The width of the tube is about 20 nm. Fig.3 (c) shows the TEM image of the sample prepared at 130 °C for 24 h. At this temperature nanotubes started to disappear. Fig.3 (d) exhibit the sample prepared at 160 °C and there is no existence of nanotubes in this system and the diameter of the particle is about 60 nm.

Figure.4 (a), (b) and (c) shows UV- spectra of prepared sample at 110°, 130°C, 160°C. The absorption onset at a) 428 nm, b) 401 nm c) 385 nm respectively. According to the Lambert–Beer's law, higher absorbance means the higher adsorption of the dye. It is well known that the photocurrent of the flexible DSSC is correlated directly with the amount of the dye molecule, the more dye molecules are adsorbed, more incident light are harvested, and the larger photocurrent occurs^{26,27}.

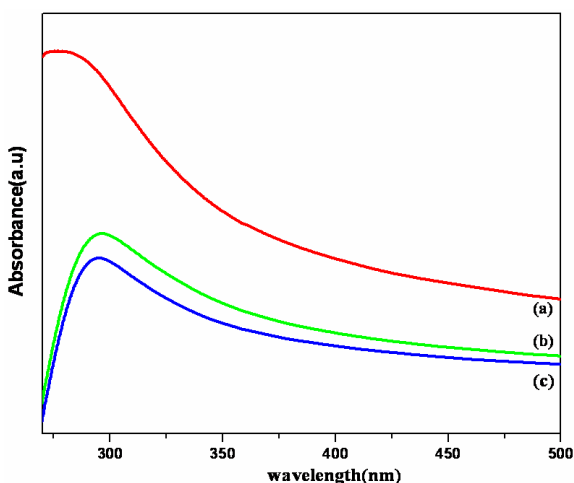


Figure.4. Shows UV- spectra of prepared sample at 110°, 130°C, 160°C

A typical isotherm for nitrogen adsorption on the surface of TiO₂ nanotube is shown in Fig.5 (a). These isotherms exhibit obvious hysteresis behavior, indicating that the products are mainly mesoporous. Basically, TiO₂ nanoparticles derived from hydrolysis methods were employed as the starting materials. The resulting nanotubes exhibited surface areas in a range of 20 and the pore volume is 0.1208 cm³/g (Inset Figure b). Since the morphology of TiO₂ m²/g nanotubes strongly depends on the size and crystalline phase of the TiO₂ source, use of the (TiO₂ nanoparticles- lab made) as the starting materials has the advantage in the property control of the nanotube products.

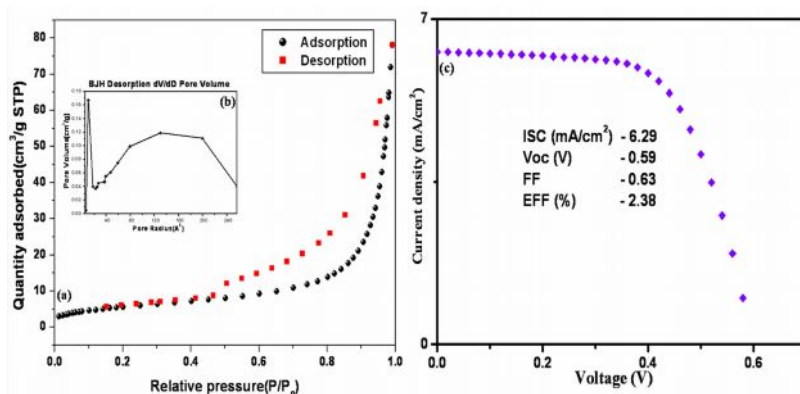


Figure.6 (a) Nitrogen adsorption–desorption isotherm and pore size distribution curve . Inset: pore diameter distribution spectra of the TiO₂ NTs. (c) I-V Characteristics of TiO₂ nanotubes prepared at 110°C.

I-V characteristics of prepared TiO₂ nanotubes are shown in fig.5 (c). TiO₂ nanotubes exhibited short circuit current densities (I_{sc}) of 6.29 mA/cm², open circuit voltages (V_{oc}) of 0.59 V, and fill factors (FF) of 0.63, respectively. The efficiency obtained for prepared TiO₂ nanotube device is 2.38 %.

4. Conclusion:

Anatase TiO₂ nanotubes with a length of 400 nm and diameter of 10 nm were prepared from synthesized TiO₂ nanoparticles using hydrothermal method. Formation of TiO₂ nanotubes were confirmed by SEM and BET surface area analysis. This method were new and cheapest method to produce nanotubes at 110° C for 24 hrs. Transformation from TiO₂ nanotube (110° C) to spherical particles (160° C) clearly revealed by TEM. Based on this result dye sensitized solar cells were fabricated for prepared TiO₂ nanotubes. The flexible DSSC with light-to-electric energy conversion efficiency of 2.38% was achieved under a simulated solar light irradiation of 100mWcm⁻².

Acknowledgement

One of the authors G.Arthi is thankful to the Shizuoka University, Research Institute of Electronics for providing necessary infrastructure to carry out this research.

References:

1. O'Regan B, Graetzel M, A Low-Cost, High-Efficiency Solar Cell Based on Dye-Sensitized Colloid TiO₂ Films, *Nature.*, 1991, 353: 737–740.
2. Kuang D, Ito S, Wenger B, Klein C, Moser JE, Humphry-Baker R, Zakeeruddin SM, Graetzel M , High Molar Extinction Coefficient Heteroleptic Ruthenium Complexes for Thin Film Dye-Sensitized Solar Cells, *Journal of the American Chemical Society.*, 2006, 128: 4146–4154.
3. Nazeeruddin MK, De Angelis F, Fantacci S, Selloni A, Viscardi G, Liska P, Ito S, Takeru B, Graetzel M, Combined Experimental and DFT-TDDFT Computational Study of Photoelectrochemical Cell Ruthenium Sensitizers, *Journal of the American Chemical Society.*, 2005, 127: 16835–16847.
4. Chiba Y, Islam A, Watanabe Y, Komiya R, Koide N, Han L , Dye-Sensitized Solar Cells with Conversion Efficiency of 11.1%, *Japanese journal of applied physics.*, 2006, 45: L638–L640.
5. Gao F, Wang Y, Shi D, Zhang J, Wang M, Jing X, Humphry-Baker R, Wang P, Zakeeruddin SM, Graetzel M, Enhance the Optical Absorptivity of Nanocrystalline TiO₂ Film with High Molar Extinction Coefficient Ruthenium Sensitizers for High Performance Dye- Sensitized Solar Cells, *Journal of the American Chemical Society.*, 2008, 130: 10720–10728.
6. Lopez-Luke T, Wolcott A, Xu LP, Chen SW, Wen ZH, Li JH, De La Rosa E, Zhang JZ, Nitrogen-Doped and CdSe Quantum-Dot-Sensitized Nanocrystalline TiO₂ Films for Solar Energy Conversion Applications, *The Journal of Physical Chemistry C.*, 2008, 112: 1282–1292.

7. Law M, Greene LE, Johnson JC, Saykally R, Yang PD, Nanowire dye-sensitized solar cells, *Nature Materials.*, 2005, 4: 455-459.
8. Zhu K, Neale NR, Miedaner A, Frank AJ, Enhanced Charge-Collection Efficiencies and Light Scattering in Dye-Sensitized Solar Cells Using Oriented TiO₂ Nanotubes Arrays, *Nano Lett.*, 2007, 7: 69–74.
9. Chen D, Zhang H, Hu S, Li JH, Preparation and Enhanced Photoelectrochemical Performance of Coupled Bicomponent ZnO–TiO₂ Nanocomposites, *The Journal of Physical Chemistry C.*, 2008, 112: 112–116.
10. Kang SH, Choi SH, Kang MS, Kim JY, Kim HS, Hyeon T, Sung YE, Nanorod-Based Dye-Sensitized Solar Cells with Improved Charge Collection Efficiency, *Advanced materials.*, 2008, 20: 54-58.
11. Yang WG, Wan FR, Wang YL, Jiang CH, Achievement Of 6.03% Conversion Efficiency Of Dye-Sensitized Solar Cells With Single-Crystalline Rutile TiO₂ Nanorod Photoanode, *Applied Physics Letters.*, 2009, 95: 133121.
12. Fujihara K, Kumar A, Jose R, Ramakrishna S, Uchida S, Spray deposition of electrospun TiO₂ nanorods for dye-sensitized solar cell, *Nanotechnology.*, 2007, 18: 365709.
13. Wang HE, Chen ZH, Leung YH, Luan CY, Liu CP, Tang YB, Yan C, Zhang WJ, Zapien JA, Bello I, Lee, ST, Hydrothermal synthesis of ordered single-crystalline rutile TiO₂ nanorod arrays on different substrates, *Applied Physics Letters.*, 2010, 96: 263104.
14. Kang TS, Smith AP, Taylor BE, Durstock MF, Fabrication of highly-ordered TiO₂ nanotube arrays and their use in dye-sensitized solar cells, *Nano letters.*, 2009, 9: 601–606.
15. Oh JK, Lee JK, Kim HS, Han SB, Park KW, TiO₂ branched nanostructure electrodes synthesized by seeding method for dye-sensitized solar cells, *Chemistry of materials.*, 2010, 22: 1114–1118.
16. Lee KM, Suryanarayanan V, Ho KC, Influences of different TiO₂ morphologies and solvents on the photovoltaic performance of dye-sensitized solar cells, *Journal of Power Sources.*, 2009, 188: 635-641.
17. Li LL, Tsai CY, Wu HP, Chen CC, Diao EWG, Fabrication of long TiO₂ nanotube arrays in a short time using a hybrid anodic method for highly efficient dye-sensitized solar cells, *Journal of Materials Chemistry.*, 2010, 20: 2753-2758.
18. Kuang D, Brillat J, Chen P, Takata M, Uchida S, Miura H, Sumioka K, Zakeeruddin SM, Gratzel M, Application of highly ordered TiO₂ nanotube arrays in flexible dye-sensitized solar cells, *ACS Nano.*, 2008, 2: 1113–1116.
19. Chun KY, Park BW, Sung YM, Kwak DJ, Hyun YT, Park MW, Fabrication of dye-sensitized solar cells using TiO₂-nanotube arrays on Ti-grid substrates, *Thin Solid Films.*, 2009, 517: 4196-4198.
20. Shankar K, Mor GK, Prakasam HE, Yoriya S, Paulose M, Varghese OK, Grimes CA, Highly-ordered TiO₂ nanotube arrays up to 220 μm in length: use in water photoelectrolysis and dye-sensitized solar cells, *Nanotechnology.*, 2007, 18: 065707.
21. Yin H, Liu H, Shen WZ, The large diameter and fast growth of self-organized TiO₂ nanotube arrays achieved via electrochemical anodization, *Nanotechnology.*, 2010, 21: 035601.
22. Lei Y, Zhang LD, Meng GW, Li GH, Zhang XY, Liang CH, Chen W, Wang SX, Preparation and photoluminescence of highly ordered TiO₂ nanowire arrays, *Applied physics letters.*, 2001, 78: 1125.
23. Attar A S, Ghamsari MS, Hajiesmaeilbaigi F, Mirdamadi S, Katagiri K, Koumoto K, Sol-gel template synthesis and characterization of aligned anatase-TiO₂ nanorod arrays with different diameter, *Materials Chemistry and Physics.*, 2009 113: 856 – 860.
24. Morgan DL, Liu HW, Frost RL, Waclawik ER, Implications of Precursor Chemistry on the Alkaline Hydrothermal Synthesis of Titania/Titanate Nanostructures, *The Journal of Physical Chemistry C.*, 2010 114: 101–110.
25. Chen Q, Du GH, Zhang S, Peng LM, The structure of trititanate nanotubes, *Acta Crst. B.*, 2002, 58: 587-593.
26. Kasuga T, Hiramatsu M, Hoson A, Sekino T, Niihara K, Formation of Titanium Oxide Nanotube, *Langmuir.*, 1998, 14: 3160–3163.
27. Seo DS, Lee JK, Kim H, Preparation of nanotube-shaped TiO₂ powder. *Journal of Crystal Growth.*, 2001, 229: 428-432.
